DOI: 10.1534/genetics.109.113613

The Influence of Horizontal Gene Transfer on the Mean Fitness of Unicellular Populations in Static Environments

Yoav Raz and Emmanuel Tannenbaum[1]

Department of Chemistry, Ben-Gurion University of the Negev, Be'er-Sheva, 84105 Israel

Manuscript received December 25, 2009
Accepted for publication February 21, 2010

ABSTRACT

Horizontal gene transfer (HGT) is believed to be a major source of genetic variation, particularly for prokaryotes. It is believed that horizontal gene transfer plays a major role in shaping bacterial genomes and is also believed to be responsible for the relatively rapid dissemination and acquisition of new, adaptive traits across bacterial strains. Despite the importance of horizontal gene transfer as a major source of genetic variation, the bulk of research on theoretical evolutionary dynamics and population genetics has focused on point mutations (sometimes coupled with gene duplication events) as the main engine of genomic change. Here, we seek to specifically model HGT processes in bacterial cells, by developing a mathematical model describing the influence that conjugation-mediated HGT has on the mutation–selection balance in an asexually reproducing population of unicellular, prokaryotic organisms. It is assumed that mutation–selection balance is reached in the presence of a fixed background concentration of antibiotic, to which the population must become resistant to survive. We find that HGT has a nontrivial effect on the mean fitness of the population. However, one of the central results that emerge from our analysis is that, at mutation–selection balance, conjugation-mediated HGT has a slightly deleterious effect on the mean fitness of a population. Therefore, we conclude that HGT does not confer a selection advantage in static environments. Rather, its advantage must lie in its ability to promote faster adaptation in dynamic environments, an interpretation that is consistent with the observation that HGT can be promoted by environmental stresses on a population.

HORIZONTAL gene transfer (HGT) is any form of direct transfer of genetic material between two organisms, where one organism is not the parent of the other (the latter case is known as *vertical gene transfer*) (Ochman *et al.* 2000; Brown 2003; Kurland *et al.* 2003; Gogarten and Townsend 2005). HGT has become a subject of great interest for both molecular and evolutionary biologists, because it is believed that HGT plays a large role in reshaping prokaryotic genomes (Ochman *et al.* 2000; Brown 2003; Kurland *et al.* 2003; Gogarten and Townsend 2005). HGT is believed to be primarily responsible for the rapid spread of antibiotic drug resistance in bacterial populations (Walsh 2000).

Currently, there are three known mechanisms by which HGT occurs (Ochman *et al.* 2000; Brown 2003; Kurland *et al.* 2003; Gogarten and Townsend 2005): (1) *transformation*, when an organism collects genetic material from its environment; (2) *transduction*, when a virus directly infiltrates a bacterium with genetic material; and (3) *bacterial conjugation*, when a bacterium transfers genetic information via intercellular contact with another bacterium.

Bacterial conjugation is believed to be the most important mechanism responsible for HGT (Ochman *et al.* 2000; Brown 2003; Kurland *et al.* 2003; Gogarten and Townsend 2005), and so we focus on developing mathematical models describing the role that conjugation-mediated HGT has on the mutation–selection balance of bacterial populations. Given the presumed importance that HGT has for the spread of antibiotic drug resistance in bacterial populations, the mathematical models we develop look at the influence of HGT on the mutation–selection balance in the presence of an antibiotic. This is not the most realistic setting in which to study HGT, since it is more relevant to look at the role that HGT plays in the evolution and spread of antibiotic drug resistance in an initially nonresistant population. Nevertheless, it is important to understand the mutation–selection balance first, since this serves as a starting point for modeling dynamics.

The best-characterized bacterial conjugation system is the F^+/F^- system (Russi *et al.* 2008). Here, a bacterium containing what is termed an *F-plasmid* fuses with a bacterium lacking the F-plasmid. The bacterium containing the F-plasmid is termed an F^+ bacterium, while the bacterium that does not contain this plasmid is termed an F^- bacterium. When the F^+ bacterium meets an F^- bacterium, it transfers one of the strands of the F-plasmid to the F^- bacterium via a *pilus*. Once a strand of the F-plasmid has been transferred from the F^+ bacterium to the F^- bacterium, a copy of the plasmid

[1]*Corresponding author:* Department of Chemistry, Ben-Gurion University of the Negev, Be'er-Sheva, 84105 Israel. E-mail: emanuelt@bgu.ac.il

in both cells is produced by daughter strand synthesis using the DNA template strands. The F^- bacterium then becomes an F^+ bacterium that transcribes its own pilus and is able to transfer the F^+ plasmid to other bacteria in the population (Russi *et al.* 2008). This process is illustrated in Figure 1.

The F^+/F^- system is in some ways atypical for bacterial conjugation systems: The F-plasmid system studied in the K12 strain of *Escherichia coli* was permanently derepressed, which meant that conjugation between F^+ and F^- cells occurred at a significantly elevated rate. Generally, conjugative plasmids tend to be repressed, so that only a small fraction of the plasmid-bearing bacterial population is able to participate in conjugation at any given time (Ghigo 2001). It is believed that this reduces the metabolic costs associated with continuously maintaining the enzymatic machinery necessary for conjugation (Ghigo 2001). Indeed, it is known that mutant forms of the F-plasmid system are permanently derepressed (Ghigo 2001), so it is possible that these are the strains that were accidentally generated under the experimental conditions that the plasmids were being studied. Nevertheless, because the F-plasmid system is one of the best-characterized bacterial conjugation systems, and because it is representative of all known bacterial conjugation systems, we believe it makes sense to base our initial model for conjugation-mediated HGT on the F-plasmid system.

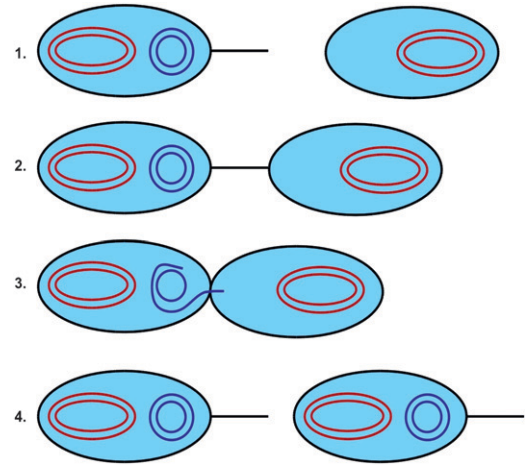

Figure 1.—Illustration of the process of bacterial conjugation. In steps 1 and 2, an F^+ bacterium containing the F-plasmid (blue) binds to an F^- bacterium lacking the plasmid. One of the template strands from the F-plasmid then moves into the F^- bacterium, as shown in step 3. In step 4, the complementary strands are synthesized to reform the complete F-plasmids in both bacteria. Both bacteria are now of the F^+ type.

METHODS

We assume that the genome of each bacterium consists of two DNA molecules. The first DNA molecule contains all of the genes necessary for the proper growth and reproduction of the bacterium itself. It corresponds to the large, circular chromosome defining the bacterial genome. We assume that there exists a wild-type genome characterized by a "master" DNA sequence. It is assumed that a bacterium with the master genome has a wild-type fitness, or first-order growth rate constant, given by 1. Such a bacterium is termed *viable*. Furthermore, we assume that any mutation to the bacterial genome renders the genome defective, so that the bacterium then has a fitness of 0. Bacteria with defective genomes are termed *nonviable*. This is known as the *single-fitness-peak approximation* in quasispecies theory (Tannenbaum and Shakhnovich 2005).

The second DNA molecule is the F-plasmid, which we assume consists of two regions. The first region comprises the various genes necessary for bacterial conjugation. The second region is assumed to encode for the various enzymes conferring resistance to a given antibiotic. As with the single-fitness-peak approximation made for the bacterial genome, we assume that there are master sequences for both the conjugation and the antibiotic drug resistance regions. If the region coding for bacterial conjugation corresponds to a given master sequence, then, assuming that the bacterium is also viable, the F-plasmid may be copied into another viable F^- bacterium. Otherwise, we assume that the plasmid cannot be copied into another bacterium, in which case the bacterium is treated as an F^- bacterium. Similarly, if the region coding for antibiotic drug resistance corresponds to a given master sequence, then we assume that the bacterium is resistant to the antibiotic. Otherwise, the bacterium is not resistant to the antibiotic and is assumed to die with a first-order rate constant κ_D. We assume that only viable bacteria interact with the antibiotic, since nonviable bacteria do not grow and so may be treated as dead.

A given viable genome may be characterized by a two-symbol sequence $\sigma = \pm\ \pm$, specifying the state of the conjugation and resistance portions of the plasmid, respectively. A "+" is taken to signify that the given genome region is identical to the corresponding master sequence, and a "−" is taken to signify that the given genome region differs from the corresponding master sequence. To develop the evolutionary dynamics equations governing this population, we let n_σ denote the number of organisms in the population with genome σ. We wish to develop expressions for dn_σ/dt for the various σ's. We do not consider nonviable genomes, since they do not reproduce or participate in the conjugation process and therefore do not contribute to the evolutionary dynamics of the population.

The semiconservative replication of the bacterial genome is not necessarily error free, so that there is a probability p, the replication fidelity, that a given template strand will produce a daughter genome that is identical to the original parent. Because our genome consists of three genome regions, we may define three

such probabilities, denoted p_v, p_c, and p_r, corresponding to the replication fidelities for the viability, conjugation, and resistance portions of the genome. If we assume that sequence lengths are long, then making an assumption known as the *neglect of back mutations* (Tannenbaum and Shakhnovich 2005), we assume that a template strand derived from a parent that differs from the master genome produces a daughter that differs from the master genome with probability 1.

We assume that conjugation occurs between a viable F^+ bacterium and a viable F^- bacterium. Thus, conjugation can occur only between a bacterium of type $+\pm$ and a bacterium of type $-\pm$. This process is modeled as a second-order collision reaction with a rate constant γ. The conjugation process itself involves the transfer of one of the strands of the plasmid from the F^+ bacterium to the F^- bacterium, so that the full plasmid needs to be resynthesized in both bacteria via daughter strand synthesis. This introduces the possibility of replication errors in either one of the bacteria.

It should be emphasized that we are assuming for simplicity that all bacteria in the population contain exactly one plasmid. We also assume that, during conjugation, the plasmid transferred from the F^+ bacterium replaces the plasmid in the F^- bacterium. This is a simplifying assumption that will obviously have to be reexamined in future research, where we anticipate developing more accurate models that allow for variable plasmid numbers in the bacterial cell. The basis for this assumption derives from the observation that plasmids of similar compatibility classes cannot coexist in the same cell (Uhlin and Nordstrom 1975) and that bacteria can control the number of plasmids in the cell (Park *et al.* 2001).

Putting everything together, we obtain that the evolutionary dynamics equations are

$$\begin{aligned}
\frac{dn_{++}}{dt} &= [2p_vp_cp_r - 1 + \frac{\gamma}{V}(2p_cp_r - 1)(n_{-+} + n_{--})]n_{++}\\
\frac{dn_{+-}}{dt} &= [2p_vp_c - 1 - \kappa_D + \frac{\gamma}{V}(2p_c - 1)(n_{-+} + n_{--})]n_{+-}\\
&\quad + 2p_c(1 - p_r)[p_v + \frac{\gamma}{V}(n_{-+} + n_{--})]n_{++}\\
\frac{dn_{-+}}{dt} &= [2p_vp_r - 1 - \frac{\gamma}{V}(n_{++} + n_{+-})]n_{-+}\\
&\quad + 2(1 - p_c)p_r[p_v + \frac{\gamma}{V}(n_{-+} + n_{--})]n_{++}\\
\frac{dn_{--}}{dt} &= [2p_v - 1 - \kappa_D - \frac{\gamma}{V}(n_{++} + n_{+-})]n_{--}\\
&\quad + 2(1 - p_c)(1 - p_r)\Big[p_v + \frac{\gamma}{V}(n_{-+} + n_{--})\Big]n_{++}\\
&\quad + 2(1 - p_c)\Big[p_v + \frac{\gamma}{V}(n_{-+} + n_{--})\Big]n_{+-}\\
&\quad + 2p_v(1 - p_r)n_{-+},
\end{aligned} \tag{1}$$

where V is defined as the system volume. To put the equations into a form that makes the analysis of the mutation–selection balance possible, we define n to be the total population of organisms and then define population fractions x_σ via $x_\sigma = n_\sigma/n$. We also define a population density $\rho = n/V$, and we assume that ρ is constant. The assumption of a constant ρ can be achieved if we assume that the system volume is not a constant, but rather grows with the population size in such a way to maintain a constant overall population density. The idea is that each cell takes up a certain amount of space, so that the total volume of the system is proportional to the total number of cells.

Converting from population numbers to population fractions, we obtain

$$\begin{aligned}
\frac{dx_{++}}{dt} &= [2p_vp_cp_r - 1 + \gamma\rho(2p_cp_r - 1)(x_{-+} + x_{--}) - \overline{\kappa}(t)]x_{++}\\
\frac{dx_{+-}}{dt} &= [2p_vp_c - 1 - \kappa_D + \gamma\rho(2p_c - 1)(x_{-+} + x_{--}) - \overline{\kappa}(t)]x_{+-}\\
&\quad + 2p_c(1 - p_r)[p_v + \gamma\rho(x_{-+} + x_{--})]x_{++}\\
\frac{dx_{-+}}{dt} &= [2p_vp_r - 1 - \gamma\rho(x_{++} + x_{+-}) - \overline{\kappa}(t)]x_{-+}\\
&\quad + 2(1 - p_c)p_r[p_v + \gamma\rho(x_{-+} + x_{--})]x_{++}\\
\frac{dx_{--}}{dt} &= [2p_v - 1 - \kappa_D - \gamma\rho(x_{++} + x_{+-}) - \overline{\kappa}(t)]x_{--}\\
&\quad + 2(1 - p_c)(1 - p_r)[p_v + \gamma\rho(x_{-+} + x_{--})]x_{++}\\
\frac{dx_{++}}{dt} &= \left[\frac{2p_vp_cp_r - 1 + 2(1 - p_v)(1 - p_c)}{2p_c - 1} - \overline{\kappa}(t)\right]x_{++},
\end{aligned} \tag{2}$$

where $\overline{\kappa}(t) = (1/n)(dn/dt) = x_{++} + x_{-+} + (1-\kappa_D)(x_{+-} + x_{--})$ is the mean fitness of the population or, equivalently, first-order growth constant of the population.

Another point to be noted from our equations is that, in their original formulation using absolute population numbers, the equations assume unrestricted exponential growth. However, when we change variables from population numbers to population fractions, then the form of the equations is identical to what would be obtained if we made a more realistic assumption that the population was growing in a chemostat (Tannenbaum and Shakhnovich 2005).

To determine the values for p_v, p_c, and p_r, we assume that daughter strand synthesis has a per-base mismatch probability ε, which incorporates all DNA error-correction mechanisms such as proofreading and mismatch repair. Because we are assuming complementary double-stranded DNA molecules, we assume that all postreplication mismatches are corrected via various lesion repair mechanisms (*e.g.*, nucleotide excision repair, NER). However, because at this stage there is no discrimination between parent and daughter strands, a mismatch either is correctly repaired with probability 1/2 or is fixed as a mutation in the genome with probability 1/2 (Voet *et al.* 2008). Thus, the net per-base mismatch probability is $\varepsilon/2$. If the total sequence length is L, then the probability of producing a mutation-free daughter from a given parent template strand is $(1 - \varepsilon/2)^L$.

If we define $\mu = L\varepsilon$, so that μ is the average number of mismatches per template strand per replication cycle, and if we assume that $L \to \infty$ while μ is held constant, then we obtain that $(1 - \varepsilon/2)^L \to e^{-\mu/2}$. For the case of

TABLE 1

A summary of the steady-state mean fitness results obtained from our model

Regime	Mean fitness
$\gamma\rho \to 0$, arbitrary κ_D	$\max\{2p_v p_r - 1, 2p_v - 1 - \kappa_D\}$
$\gamma\rho \to \infty$, arbitrary κ_D	$\max\left\{\frac{2p_v p_c p_r - 1 + 2(1-p_v)(1-p_c)}{2p_c - 1}, 2p_v - 1 - \kappa_D\right\}$
$\kappa_D \to 0$	$2p_v - 1$
$\gamma\rho \leq (\gamma\rho)_{trans}$, $\kappa_D \to \infty$	$2p_v p_r - 1$
$\gamma\rho \to \infty$, $\kappa_D \to \infty$, finite $\gamma\rho$ regime	$\frac{2p_v p_c p_r - 1 + 2p_r(1-p_v)(1-p_c)}{1 - 2p_r(1-p_c)}$
$\gamma\rho/\kappa_D \to 0$, $\gamma\rho$, $\kappa_D \to \infty$	$\frac{2p_v p_c p_r - 1 + 2p_r(1-p_v)(1-p_c)}{1 - 2p_r(1-p_c)}$
$\gamma\rho/\kappa_D \to \infty$, $\gamma\rho$, $\kappa_D \to \infty$	$\frac{2p_v p_c p_r - 1 + 2(1-p_v)(1-p_c)}{2p_c - 1}$

the three-gene model we are considering, we let L_v, L_c, and L_r denote the lengths of the genome controlling viability, conjugation, and resistance, respectively. Defining $L = L_v + L_c + L_r$ and $\alpha_v = L_v/L$, $\alpha_c = L_c/L$, and $\alpha_r = L_r/L$, we then obtain that

$$\begin{aligned} p_v &= e^{-\alpha_v \mu/2} \\ p_c &= e^{-\alpha_c \mu/2} \\ p_r &= e^{-\alpha_r \mu/2}. \end{aligned} \tag{3}$$

It should be noted that holding μ constant in the limit of infinite genome length is equivalent to assuming a fixed per genome replication fidelity in the limit of long genomes.

RESULTS AND DISCUSSION

We present the mean fitness at mutation–selection balance, denoted by $\bar{\kappa}$, for two different sets of parameter regimes: (1) arbitrary κ_D, but with $\gamma\rho \to 0$ and $\gamma\rho \to \infty$, and (2) arbitrary $\gamma\rho$, but with $\kappa_D \to 0$ and $\kappa_D \to \infty$.

Details of the derivations of the various results are in the APPENDIX.

Behavior of $\bar{\kappa}$ for arbitrary κ_D: The steady-state mean fitnesses for arbitrary κ_D for the $\gamma\rho \to 0, \infty$ cases are provided in Table 1. We can show that $\bar{\kappa}_{\gamma\rho\to\infty} < \bar{\kappa}_{\gamma\rho\to 0}$.

Figure 2 shows plots of $\bar{\kappa}$ *vs.* μ for both the $\gamma\rho \to 0$ and the $\gamma\rho \to \infty$ limits. Plots were obtained using both the analytical formulas obtained in this article, as well as via stochastic simulations of replicating organisms.

Behavior of $\bar{\kappa}$ for arbitrary $\gamma\rho$: Now we consider the behavior of $\bar{\kappa}$ for arbitrary values of $\gamma\rho$, but where κ_D is either very small or very large. Combined with the results of the previous subsection, we may then piece together a qualitative sketch of how $\bar{\kappa}$ depends on κ_D and $\gamma\rho$.

$\kappa_D \to 0$: When $\kappa_D \to 0$, there is no selective advantage for maintaining antibiotic drug resistance genes in the genome, and so we expect these genes to be lost to genetic drift. Thus, we expect, at mutation–selection balance, that $x_{++} = x_{-+} = 0$. From Table 1, we also have that $\bar{\kappa} = 2p_v - 1$.

Furthermore, the fraction of viable conjugators, $x_{++} + x_{+-}$, exhibits a transition as a function of $\gamma\rho$. For sufficiently small values of $\gamma\rho$, we have that $x_{++} + x_{+-} = 0$, while for sufficiently large values of $\gamma\rho$, we have that

$$x_{++} + x_{+-} = 2p_v - 1 - \frac{2p_v(1-p_c)}{\gamma\rho(2p_c - 1)}. \tag{4}$$

The transition between the two regimes may be shown to occur at

$$(\gamma\rho)_{trans} \equiv \frac{2p_v(1-p_c)}{(2p_v - 1)(2p_c - 1)}. \tag{5}$$

It may be shown that the disappearance of the conjugators below the critical value of $\gamma\rho$ corresponds to a localization to delocalization transition over the portion of the plasmid coding for conjugation, so that this transition is a conjugation-mediated HGT analog of the well-known error catastrophe from quasispecies theory (TANNENBAUM and SHAKHNOVICH 2005).

To understand this behavior, we note that plasmids with defective genes for conjugation nevertheless replicate due to the replication of the bacteria in which they reside. Thus, for plasmids with functional genes for conjugation to be preserved in the population, their additional growth rate due to conjugation must overcome the loss of functionality due to replication mistakes in the genes controlling conjugation. If the conjugation rate is too slow and unable to overcome this loss of functionality, then the fraction of conjugators in the population drops to zero.

Figure 3 illustrates the regimes, as a function of μ and $\gamma\rho$, where a positive fraction of conjugators exist at steady state and where the fraction of conjugators is

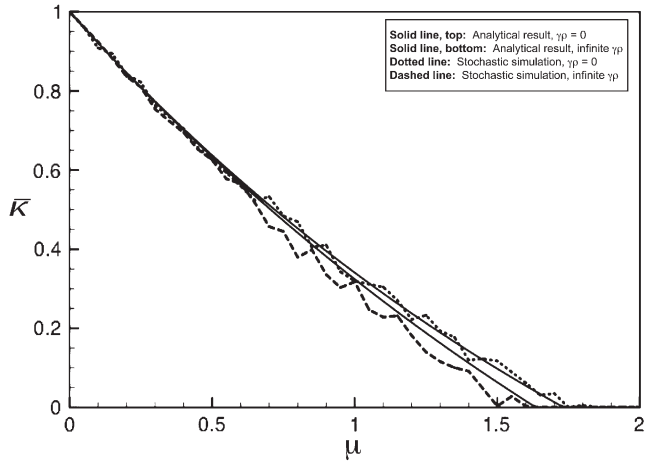

FIGURE 2.—Plots of $\bar{\kappa}$ *vs.* μ for both the $\gamma\rho \to 0$ and the $\gamma\rho \to \infty$ limits. The parameter values we took are $\alpha_v = 0.6$, $\alpha_c = \alpha_r = 0.2$, and $\kappa_D = 10$. We show both analytical results and results from stochastic simulations. The analytical results are plotted using thin solid lines, where the top curve corresponds to the $\gamma\rho = 0$ result, while the bottom curve corresponds to the $\gamma\rho = \infty$ result. The dotted line corresponds to the stochastic simulation for $\gamma\rho = 0$, and the dashed line corresponds to the stochastic simulation for $\gamma\rho = \infty$. Parameter values for the stochastic simulations were $L_v = 30$, $L_c = L_r = 10$, and a population size of 1000.

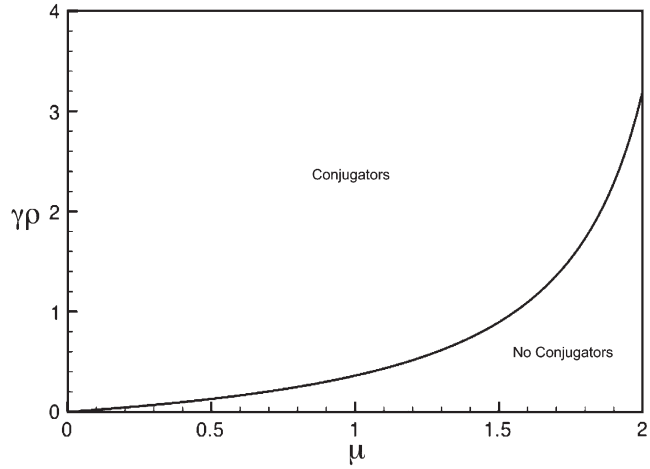

FIGURE 3.—Regimes of existence and nonexistence of conjugators as a function of μ and $\gamma\rho$, where $\kappa_D = 0$. The boundary between the two regimes was computed analytically.

zero. This is computed for the $\kappa_D = 0$ limit. Note that, as μ increases, $\gamma\rho$ must be pushed to higher values so that there is a positive fraction of conjugators at steady state. As explained before, this increase in $\gamma\rho$ is necessary to overcome the mutation-induced loss of functionality as μ increases.

$\kappa_D \to \infty$*:* We now consider the case where $\kappa_D \to \infty$. In contrast to the case where $\gamma\rho \to \infty$ of the previous subsection, where we could solve for $\bar{\kappa}$ for arbitrary values of κ_D, here we cannot readily analytically solve for $\bar{\kappa}$ for arbitrary values of $\gamma\rho$. However, we can obtain analytical solutions for $\bar{\kappa}$ in certain limiting cases of $\gamma\rho$ and then interpolate between the two solution regimes. As will be seen in the subsection comparing theory and simulation, this approach turns out to be fairly accurate.

In the first limiting case, we assume that $\gamma\rho$ remains finite in the limit that $\kappa_D \to \infty$. This ensures that $x_{+-} = x_{--} = 0$, since the rate of death due to the presence of antibiotics is so fast that no nonresistant genotypes are present in the population.

We then obtain either that $\bar{\kappa} = 2p_v p_r - 1$ or that $\bar{\kappa}$ is the solution to the following equation:

$$\gamma\rho = \frac{2(1-p_r)}{2p_c p_r - 1}\frac{\bar{\kappa} + 2(1-p_v)}{\bar{\kappa}} \times \frac{(\bar{\kappa} + 1 - 2p_v p_c p_r)^2}{[1-2p_r(1-p_c)]\bar{\kappa} - [2p_v p_c p_r - 1 + 2p_r(1-p_v)(1-p_c)]}. \quad (6)$$

In the first case, we have that $x_{++} = 0$, while in the second case we have that $x_{++} > 0$. The transition between the two regimes may be shown to occur at

$$(\gamma\rho)_{\text{trans}} = \frac{2p_v p_r(1-p_c)[1-2p_v(1-p_r)]}{(2p_v p_r - 1)(2p_c p_r - 1)}. \quad (7)$$

where $x_{++} = 0$ for $\gamma\rho \le (\gamma\rho)_{\text{trans}}$ and $x_{++} > 0$ for $\gamma\rho > (\gamma\rho)_{\text{trans}}$. We may show that this expression for $(\gamma\rho)_{\text{trans}}$ is larger than the corresponding expression for the $\kappa_D = 0$ case.

To understand the behavior of $\bar{\kappa}$ where $\gamma\rho > (\gamma\rho)_{\text{trans}}$, we consider the asymptotic behavior of $\bar{\kappa}$ in the limit as $\gamma\rho \to \infty$. In this case, Equation 6 reduces to

$$\bar{\kappa} = \frac{2p_v p_c p_r - 1 + 2p_r(1-p_v)(1-p_c)}{1 - 2p_r(1-p_c)}. \quad (8)$$

We may show that this expression is smaller than the expression for $\bar{\kappa}$ obtained in the arbitrary κ_D, infinite $\gamma\rho$ case.

We now consider the second limiting case in the $\kappa_D \to \infty$ limit, specifically where $\gamma\rho$ is itself infinite. Here, however, the ratio between κ_D and $\gamma\rho$ plays an important role in the competition between death of nonresistant bacteria and their "rescue" by conjugation with resistant bacteria. Thus, here, we assume that both $\gamma\rho$, $\kappa_D \to \infty$, but we take $\gamma\rho/\kappa_D$ to have some given value in this limit.

We may show that

$$\frac{\gamma\rho}{\kappa_D} = \frac{\bar{\kappa} + 2(1-p_v)}{\bar{\kappa}} \times \frac{[1-2p_r(1-p_c)]\bar{\kappa} - [2p_v p_c p_r - 1 + 2p_r(1-p_v)(1-p_c)]}{[2p_v p_c p_r - 1 + 2(1-p_v)(1-p_c)] - (2p_c - 1)\bar{\kappa}} \quad (9)$$

and so obtain that

$$\bar{\kappa}_{\gamma\rho/\kappa_D \to 0} = \frac{2p_v p_c p_r - 1 + 2p_r(1-p_v)(1-p_c)}{1 - 2p_r(1-p_c)}$$
$$\bar{\kappa}_{\gamma\rho/\kappa_D \to \infty} = \frac{2p_v p_c p_r - 1 + 2(1-p_v)(1-p_c)}{2p_c - 1}. \quad (10)$$

Therefore, for large κ_D, we expect that $\bar{\kappa}$ will initially be given by $2p_v p_r - 1$ up to a critical value of $\gamma\rho$, after which

it begins to decrease according to Equation 6. Once $\gamma\rho$ becomes sufficiently large, we expect that the $\gamma\rho/\kappa_D$ ratio is such that the functional form for $\bar{\kappa}$ transitions from the finite $\gamma\rho$ solution to the infinite $\gamma\rho$, fixed $\gamma\rho/\kappa_D$ solution. To estimate the transition point between the two solution regimes, we equate the values for $\gamma\rho$ as a function of $\bar{\kappa}$ for the two solutions. This allows us to solve for $\bar{\kappa}$ and thereby allows us to solve for $\gamma\rho$.

We then obtain that the transition point occurs at

$$\left(\frac{\gamma\rho}{\sqrt{\kappa_D}}\right)_{\text{trans}} = 2p_r \frac{2p_c p_r - 1 + 2(1-p_v)(1-p_r)}{2p_v p_c p_r - 1 + 2p_r(1-p_v)(1-p_c)} \times \sqrt{\frac{p_v(1-p_c)}{1-2p_r(1-p_c)}}. \quad (11)$$

Note that, as $\kappa_D \to \infty$, we have that $(\gamma\rho)_{\text{trans}} \to \infty$ and $(\gamma\rho/\kappa_D)_{\text{trans}} \to 0$, so the assumptions that allowed us to make the calculation above are valid.

Figure 4 shows three plots of $\bar{\kappa}$ *vs.* $\gamma\rho$ for $\kappa_D = 10$. One of the plots was obtained by numerically solving for the mutation–selection balance using fixed-point iteration. The other two plots correspond to the infinite κ_D, finite $\gamma\rho$ and infinite κ_D, fixed $\gamma\rho/\kappa_D$ expressions for $\bar{\kappa}$ given in the preceding subsections. Note that already for $\kappa_D = 10$ the approximate analytical solutions capture the dependence of $\bar{\kappa}$ on $\gamma\rho$ fairly accurately.

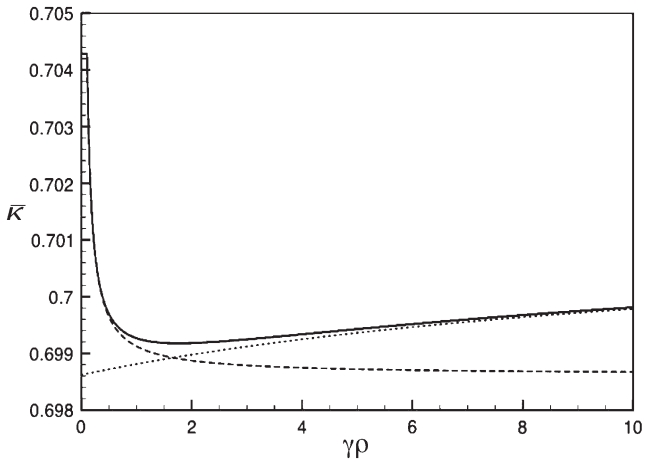

FIGURE 4.—Plots of $\bar{\kappa}$ *vs.* $\gamma\rho$ for $\kappa_D = 10$, $\mu = 0.4$, $\alpha_v = 0.6$, $\alpha_c = \alpha_r = 0.2$. The plot marked with the solid line was obtained by numerically solving for $\bar{\kappa}$ using fixed-point iteration. The dashed line was obtained by using the infinite κ_D, finite $\gamma\rho$ expression for $\bar{\kappa}$, while the dotted line was obtained by using the infinite κ_D, fixed $\gamma\rho/\kappa_D$ expression for $\bar{\kappa}$.

Conclusions: We developed a mathematical model describing the role that conjugation-mediated HGT has on the mutation–selection balance of a unicellular, asexually reproducing, prokaryotic population. We found that, in a static environment at mutation–selection balance, conjugation actually reduces the mean fitness of the population. However, by studying the dependence of the mean fitness on $\gamma\rho$ for large values of κ_D, the antibiotic-induced first-order death rate constant, we find that the behavior is somewhat more complicated: For small values of $\gamma\rho$, the mean fitness is constant, and the fraction of viable conjugators in the population is 0. At a critical value of $\gamma\rho$, the fraction of viable conjugators begins to increase, and the mean fitness decreases to its minimum value. After reaching its minimum, the mean fitness increases asymptotically to the $\gamma\rho \to \infty$ limit, which is nevertheless smaller than the small $\gamma\rho$ value for the mean fitness. We developed approximate analytical solutions for the functional dependence of the mean fitness on $\gamma\rho$ in the limit of large κ_D and found that these solutions agree well with simulation. Although the fitness variations as a function of $\gamma\rho$ were fairly small for the parameter values studied, we believe that this is nontrivial behavior that is important to characterize.

Although the results of our article are based on a highly simplified model, they nevertheless suggest that HGT does not provide a selective advantage in a static environment. This is likely due to the fact that, due to mutation, HGT can destroy antibiotic drug resistance in a previously resistant cell. While HGT can also confer resistance to a nonresistant cell, natural selection alone is sufficient to maximize the population mean fitness in a static environment. HGT simply has the net effect of destroying favorable genes, thereby lowering the mean fitness. This result may be viewed as an example of the "If it is not broken, do not fix it" principle.

Thus, on the basis of the results of this article, we argue that HGT likely has a selective advantage only in dynamic environments, where it would act to speed up rates of adaptation. While this result needs to be checked in future research, it is nevertheless consistent with the observation that bacteria can regulate their rates of HGT. For example, it is known that, in response to stress, bacteria can activate the SOS response (Beaber *et al.* 2004), which has the effect of increasing rates of HGT. It is also suspected that bacteria can increase their mutation rates in response to stress (Bjedov *et al.* 2003), which, coupled with the observation that mismatch-repair-deficient cells, or mutators, have significantly increased rates of recombination and HGT (Denamur *et al.* 2000), suggests that there is a strong correlation between HGT, stress, and adaptation. This is consistent with our results suggesting that HGT should be kept at a minimal level in static environments and increased in dynamic environments. It is also worth mentioning that while conjugation-mediated HGT has not been specifically modeled before in this manner (at least to our knowledge), other HGT-like models have been studied (Cohen *et al.* 2005; Park and Deem 2007), and these studies have found that HGT does indeed allow for faster adaptation in dynamic environments (Cohen *et al.* 2005).

It should be noted that we have obtained our conclusions by an analysis of the mean fitness of the population. Thus, our analysis is based on what is known as a

group selection approach, whereby we assume that what is beneficial for the population as a whole dictates what will actually be observed. The group selection approach is known to have some serious drawbacks, specifically because it cannot explicitly account for selfish behavior such as defection from a cooperative strategy or independently replicating entities that act as parasites on a larger host system (the plasmids may be viewed as such an example).

However, in a certain sense, even analyses based on individual-selection models are themselves group selection approaches. For example, in analyzing the dynamics of defection and cooperation, one looks at the rate of growth of defectors *vs.* the rate of growth of cooperators. If, by group selection, one means that the mean fitness of the entire population is used to determine the structure of the mutation–selection balance, then indeed this approach will fail to give the correct results. However, if two mean fitnesses are used, one for the defectors and one for the cooperators, then the resulting analysis will capture the coevolutionary dynamics between cooperators and defectors in the correct manner. Similarly, when dealing with host–parasite interactions, one does not simply consider the mean fitness of the host and study the influence that the parasites have on the host fitness. Rather, one works with mathematical models that consider both the host and the parasite fitnesses, which again leads to a coevolutionary dynamics that can lead to correct results. This is the approach one must take when dealing with plasmid–bacteria systems or with viral–bacteria systems.

Given the discussion in the above paragraph, it may then appear that there is something contradictory between the analysis we stated should be done on bacteria–plasmid systems and the analysis that we actually carried out. To resolve this, we must emphasize that the purpose of this article is not to characterize the coevolutionary dynamics of bacteria and plasmids. Rather, the purpose is to determine what effect the presence of plasmids and, in particular, the presence of plasmids that confer some selective advantage to the bacterial hosts (*e.g.*, drug resistance) has on the overall fitness of a population of bacteria in a static environment. As stated, we find that the mean fitness has nontrivial aspects to its behavior, but the central result is that plasmids capable of moving between bacteria via conjugation actually have a deleterious effect on fitness in a static environment.

This in no way suggests that plasmids will therefore not undergo conjugation, since, as selfish genetic elements residing within bacterial cells, they are under a selection pressure to evolve a conjugation ability even if they negatively affect bacterial fitness (the case of viruses in the lytic phase makes this point very obvious). However, to the extent that bacteria can control rates of conjugation, the results of this article suggest that, in a static environment at mutation–selection balance, bacteria have an "interest" in keeping rates of conjugation as low as possible, as long as the costs associated with such control mechanisms are not prohibitive. This is consistent with the observation that HGT can become significantly elevated in response to stress.

There are several extensions of the model that should be considered in future research: First, we need to model the role that HGT plays in adaptive dynamics. Second, we need to develop more realistic models for the conjugation process itself. This includes moving away from the single-plasmid-per-bacterium model considered here and to actually model plasmid compatibility classes and the regulation of copy number inside bacterial cells. This also includes properly modeling the repression/derepression dynamics associated with the activation of the conjugation process itself. Third, our current model assumes that all plasmids have identical characteristics. This does not take into account that, in many models of recombination, a modifier allele that allows for cell-specific recombination rates is often considered and that the evolution of the recombination rate itself is often modeled. Such models will be useful to determine the optimal level of horizontal gene transfer in various environments and to understand the distribution of horizontal gene transfer rates in bacterial populations.

Finally, and perhaps most importantly, it is important to carry out experimental studies to see if the qualitative predictions made as to how the mean fitness of the population varies as a function of conjugation rate are correct. We believe that the existing model may be relevant for plasmid systems that have low copy number in their host cells. Recent work (Barrick *et al.* 2009) points to the kinds of experimental studies in this area that are desired.

LITERATURE CITED

Barrick, J. E., D. S. Yu, S. H. Yoon, H. Jeong, T. K. Oh *et al.*, 2009 Genome evolution and adaptation in a long-term experiment with Escherichia coli. Nature **461:** 1243–1247.

Beaber, J. W., B. Hochhut and M. K. Waldor, 2004 SOS response promotes horizontal dissemination of antibiotic resistance genes. Nature **427:** 72–74.

Bjedov, I., O. Tenaillon, B. Gerard, V. Souza, E. Denamur *et al.*, 2003 Stress-induced mutagenesis in bacteria. Science **300:** 1404–1409.

Brown, J. R., 2003 Ancient horizontal gene transfer. Nat. Rev. Genet. **4:** 121–132.

Cohen, E., D. A. Kessler and H. Levine, 2005 Recombination dramatically speeds up evolution of finite populations. Phys. Rev. Lett. **94:** 098102.

Denamur, E., G. Lecointre, P. Darlu, O. Tenaillon, C. Acquaviva *et al.*, 2000 Evolutionary implications of the frequent horizontal transfer of mismatch repair genes. Cell **103:** 711–721.

Ghigo, J. M., 2001 Natural conjugative plasmids induce bacterial biofilm development. Nature (Lond.) **412:** 442–445.

Gogarten, J. P., and J. P. Townsend, 2005 Horizontal gene transfer, genome innovation, and evolution. Nat. Rev. Microbiol. **3:** 679–687.

Kurland, C. G., B. Canback and O. G. Berg, 2003 Horizontal gene transfer: A critical view. Proc. Natl. Acad. Sci. USA **100:** 9658–9662.

Ochman, H., J. G. Lawrence and E. A. Groisman, 2000 Lateral gene transfer and the nature of bacterial innovation. Nature (Lond.) **405:** 299–304.

Park, J. M., and M. W. Deem, 2007 Phase diagrams of quasispecies theory with recombination and horizontal gene transfer. Phys. Rev. Lett. **98:** 058101.

Park, K., E. Han, J. Paulsson and D. K. Chattoraj, 2001 Origin pairing ("handcuffing") as a mode of negative control of P1 plasmid copy number. EMBO J. **20:** 7323–7332.

Russi, S., R. Boera and M. Coll, 2008 Molecular machinery for DNA translocation in bacterial conjugation, pp. 183–214 in *Plasmids: Current Research and Future Trends*, edited by G. Lipps. Caister Academic Press, Cambridge, UK.

Tannenbaum, E., and E. I. Shakhnovich, 2005 Semiconservative replication, genetic repair, and many-gened genomes: extending the quasispecies paradigm to living systems. Phys. Life Rev. **2:** 290–317.

Uhlin, B. E., and K. Nordstrom, 1975 Plasmid incompatibility and control of replication: copy mutants of the R-factor R1 in Escherichia coli K-12. J. Bacteriol. **124:** 641–649.

Voet, D., J. G. Voet and C. W. Pratt, 2008 *Fundamentals of Biochemistry: Life at the Molecular Level*, Ed. 3. Wiley, New York.

Walsh, C., 2000 Molecular mechanisms that confer antibacterial drug resistance. Nature (Lond.) **406:** 775–781.

Communicating editor: M. W. Feldman

APPENDIX: DERIVATION DETAILS OF THE ANALYTICAL RESULTS

Derivation of $\bar{\kappa}$ for arbitrary κ_D and $\gamma\rho \to 0$: Due to the nature of exponential growth, for the population fractions to converge to a stable steady state we must have that $\bar{\kappa} \geq 2p_v p_c p_r - 1,\ 2p_v p_c - 1 - \kappa_D,\ 2p_v p_r - 1,\ 2p_v - 1 - \kappa_D$. Because $2p_v p_c p_r - 1 < 2p_v p_r - 1$ and $2p_v p_c - 1 - \kappa_D < 2p_v - 1 - \kappa_D$, it follows that $\bar{\kappa} \geq 2p_v p_r - 1,\ 2p_v - 1 - \kappa_D$. However, if we then look at the steady-state version of Equation 2, obtained by setting the time derivatives to 0, we then obtain that $x_{++} = x_{+-} = 0$. If $x_{-+} > 0$, then the third equation gives us that $\bar{\kappa} = 2p_v p_r - 1$; otherwise the fourth equation gives us $\bar{\kappa} = 2p_v - 1 - \kappa_D$.

So, we have shown that $\bar{\kappa} \geq 2p_v p_r - 1,\ 2p_v - 1 - \kappa_D$, and yet $\bar{\kappa} = 2p_v p_r - 1$ or $2p_v - 1 - \kappa_D$. These two requirements imply that $\bar{\kappa} = \max\{2p_v p_r - 1,\ 2p_v - 1 - \kappa_D\}$. Note that we have also shown that $x_{++} + x_{+-} = 0$, so that our claim that conjugation is lost due to genetic drift has also been proven.

Derivation of $\bar{\kappa}$ for arbitrary κ_D and $\gamma\rho \to \infty$: In the limit where $\gamma\rho \to \infty$, we have that $x_{-+} = x_{--} = 0$. However, $\gamma\rho x_{-+}$ and $\gamma\rho x_{--}$ may converge to positive values. So, we define $z_{-+} = \gamma\rho x_{-+}$ and $z_{--} = \gamma\rho x_{--}$.

Because $x_{-+} = x_{--} = 0$, we also have that $dx_{-+}/dt = dx_{--}/dt = 0$, and so from Equation 2 we have that

$$\begin{aligned} 0 = &-z_{-+}(x_{++} + x_{+-}) + 2(1 - p_c)\left[p_v + z_{-+} + z_{--}\right]p_r x_{++} 0 = -z_{--}(x_{++} + x_{+-}) \\ &+ 2(1 - p_c)\left[p_v + z_{-+} + z_{--}\right]\left[(1 - p_r)x_{++} + x_{+-}\right]. \end{aligned} \tag{A1}$$

Summing these two equations and solving for $z_{-+} + z_{--}$ gives

$$z_{-+} + z_{--} = \frac{2(1 - p_c)p_v}{2p_c - 1}. \tag{A2}$$

Substituting into the expressions for dx_{++}/dt and dx_{+-}/dt from Equation 2 we obtain, after some manipulation,

$$\begin{aligned} \frac{dx_{++}}{dt} &= \left[\frac{2p_v p_c p_r - 1 + 2(1 - p_v)(1 - p_c)}{2p_c - 1} - \bar{\kappa}(t)\right]x_{++} \\ \frac{dx_{+-}}{dt} &= \left[2p_v - 1 - \kappa_D - \bar{\kappa}(t)\right]x_{+-} + \frac{2p_v p_c(1 - p_r)}{2p_c - 1}x_{++}. \end{aligned} \tag{A3}$$

Following a similar argument to the $\gamma\rho \to 0$ case, we obtain the expression for $\bar{\kappa}_{\gamma\rho\to\infty}$ given in the main text.

To prove that $\bar{\kappa}_{\gamma\rho\to\infty} < \bar{\kappa}_{\gamma\rho\to 0}$, we need only show that

$$\frac{2p_v p_c p_r - 1 + 2(1 - p_v)(1 - p_c)}{2p_c - 1} < 2p_v p_r - 1. \tag{A4}$$

After some manipulation, it may be shown that this inequality is equivalent to $p_r < 1$, which clearly holds, thereby proving the claim.

Derivation of $\bar{\kappa}$ for $\kappa_D \to 0$ and arbitrary $\gamma\rho$: We can add the first two equations from Equation 2, and also the third and fourth equations, to obtain the pair of equations

$$\begin{aligned} \frac{d(x_{++} + x_{+-})}{dt} &= [2p_v p_c - 1 + \gamma\rho(2p_c - 1)(x_{-+} + x_{--}) - \bar{\kappa}(t)](x_{++} + x_{+-}) \\ \frac{d(x_{-+} + x_{--})}{dt} &= [2p_v - 1 - \gamma\rho(x_{++} + x_{+-}) - \bar{\kappa}(t)](x_{-+} + x_{--}) \\ &\quad + 2(1 - p_c)[p_v + \gamma\rho(x_{-+} + x_{--})](x_{++} + x_{+-}). \end{aligned} \tag{A5}$$

Summing these two equations then gives

$$\frac{d(x_{++}+x_{+-}+x_{-+}+x_{--})}{dt}=[2p_v-1-\overline{\kappa}(t)](x_{++}+x_{+-}+x_{-+}+x_{--}) \tag{A6}$$

from which it follows that $\overline{\kappa}=2p_v-1$ at steady state.

Substituting this value for $\overline{\kappa}$ into the steady-state version of Equation A5, we obtain

$$0=[(2p_c-1)\gamma\rho(x_{-+}+x_{--})-2p_v(1-p_c)](x_{++}+x_{+-}), \tag{A7}$$

which gives either that $x_{++}+x_{+-}=0$ or that $x_{-+}+x_{--}=2p_v(1-p_c)/[\gamma\rho(2p_c-1)]$. If the second case holds, then since $2p_v-1=\overline{\kappa}=x_{++}+x_{+-}+x_{-+}+x_{--}$, we obtain that

$$x_{++}+x_{+-}=2p_v-1-\frac{2p_v(1-p_c)}{\gamma\rho(2p_c-1)}. \tag{A8}$$

Now, for large values of $\gamma\rho$, we expect that the population will consist of a nonzero fraction of conjugators, so that $x_{++}+x_{+-}>0$. However, because $x_{++}+x_{+-}$ cannot be negative, we must have that

$$\gamma\rho\geq(\gamma\rho)_{\text{trans}}\equiv\frac{2p_v(1-p_c)}{(2p_v-1)(2p_c-1)} \tag{A9}$$

for $x_{++}+x_{+-}\geq 0$. Therefore, by continuity, we expect that $x_{++}+x_{+-}=0$ for $\gamma\rho\leq(\gamma\rho)_{\text{trans}}$ and $x_{++}+x_{+-}=2p_v-1-2p_v(1-p_c)/\gamma\rho(2p_c-1)>0$ for $\gamma\rho>(\gamma\rho)_{\text{trans}}$.

Derivation of $\overline{\kappa}$ for $\kappa_D\to\infty$ and finite $\gamma\rho$: In this limiting case, although $x_{+-}=x_{--}=0$, it is possible that $y_{+-}\equiv\kappa_D x_{+-}$ and $y_{--}\equiv\kappa_D x_{--}$ have nonzero, finite values in the limit as $\kappa_D\to\infty$, and so we need to consider the effect of these quantities in our analysis. We then have that the steady-state version of Equation 2 reads

$$\begin{aligned}
0&=[2p_vp_cp_r-1+\gamma\rho(2p_cp_r-1)x_{-+}-\overline{\kappa}]x_{++}\\
0&=[2p_vp_r-1-\gamma\rho x_{++}-\overline{\kappa}]x_{-+}+2(1-p_c)p_r[p_v+\gamma\rho x_{-+}]x_{++}\\
y_{+-}&=2p_c(1-p_r)[p_v+\gamma\rho x_{-+}]x_{++}\\
y_{--}&=2(1-p_c)(1-p_r)[p_v+\gamma\rho x_{-+}]x_{++}+2p_v(1-p_r)x_{-+}.
\end{aligned} \tag{A10}$$

If $x_{++}=0$ at steady state, then $\overline{\kappa}=2p_vp_r-1$. So, let us consider the case where $x_{++}>0$. Summing the first two equations from Equation A10 gives

$$2(1-p_r)\gamma\rho x_{++}x_{-+}=[2p_vp_r-1-\overline{\kappa}](x_{++}+x_{-+}). \tag{A11}$$

Summing the last two equations from Equation A10 then gives

$$y_{+-}+y_{--}=[2p_v-1-\overline{\kappa}](x_{++}+x_{-+}). \tag{A12}$$

Now, in the limiting case being considered here, we have that $\overline{\kappa}=x_{++}+x_{-+}-y_{+-}-y_{--}=[\overline{\kappa}+2(1-p_v)](x_{++}+x_{-+})$, and so,

$$x_{++}+x_{-+}=\frac{\overline{\kappa}}{\overline{\kappa}+2(1-p_v)}. \tag{A13}$$

Since $x_{++}>0$, the first equation from Equation A10 gives

$$x_{-+}=\frac{\overline{\kappa}+1-2p_vp_cp_r}{\gamma\rho(2p_cp_r-1)}, \tag{A14}$$

and so,

$$x_{++}=\frac{\overline{\kappa}}{\overline{\kappa}+2(1-p_v)}-\frac{\overline{\kappa}+1-2p_vp_cp_r}{\gamma\rho(2p_cp_r-1)}. \tag{A15}$$

Substituting into Equation A11 gives the following nonlinear equation that $\overline{\kappa}$ must satisfy,

$$2(1-p_r)\frac{\overline{\kappa}+1-2p_vp_cp_r}{2p_cp_r-1}\left[\frac{\overline{\kappa}}{\overline{\kappa}+2(1-p_v)}-\frac{\overline{\kappa}+1-2p_vp_cp_r}{\gamma\rho(2p_cp_r-1)}\right]$$
$$=\frac{\overline{\kappa}}{\overline{\kappa}+2(1-p_v)}[2p_vp_r-1-\overline{\kappa}], \tag{A16}$$

which, after some manipulation, may be shown to be equivalent to Equation 6.

To determine the critical value for the transition between the $x_{++}=0$ and the $x_{++}>0$ regimes, we note that if x_{++} is continuous at this transition, then we must have that $x_{++}=0$ using the expression in Equation A15, which gives that $\overline{\kappa}=2p_vp_r-1$ from Equation A16, so that $\overline{\kappa}$ is also continuous at this transition. Solving for the critical value of $\gamma\rho$ then gives

$$(\gamma\rho)_{\text{trans}}=\frac{2p_vp_r(1-p_c)[1-2p_v(1-p_r)]}{(2p_vp_r-1)(2p_cp_r-1)}. \tag{A17}$$

So, for $\gamma\rho\le(\gamma\rho)_{\text{trans}}$, we have that $x_{++}=0$ and $\overline{\kappa}=2p_vp_r-1$, while for $\gamma\rho>(\gamma\rho)_{\text{trans}}$ we have that $x_{++}>0$ and $\overline{\kappa}$ is given by the solution to Equation 8 or, equivalently, Equation A16.

To show that this value for $(\gamma\rho)_{\text{trans}}$ is larger than the corresponding value obtained for $\kappa_D=0$, we need to show that

$$\frac{2p_vp_r(1-p_c)[1-2p_v(1-p_r)]}{(2p_vp_r-1)(2p_cp_r-1)}>\frac{2p_v(1-p_c)}{(2p_v-1)(2p_c-1)}. \tag{A18}$$

After some manipulation, this inequality may be shown to be equivalent to

$$4p_vp_r(2p_c-1)(1-p_v)+2p_vp_r-1>0, \tag{A19}$$

which clearly holds, and so the inequality is established.

Finally, to show that the value of $\overline{\kappa}$ as $\gamma\rho\to\infty$ is smaller than the value of $\overline{\kappa}$ obtained in the arbitrary κ_D, $\gamma\rho\to\infty$ limit, we need to show that

$$\frac{2p_vp_cp_r-1+2p_r(1-p_v)(1-p_c)}{1-2p_r(1-p_c)}<\frac{2p_vp_cp_r-1+2(1-p_v)(1-p_c)}{2p_c-1}. \tag{A20}$$

After some manipulation, this condition may be shown to be equivalent to

$$p_v(2p_cp_r-1)(1-p_c)(1-p_r)>0, \tag{A21}$$

which establishes the inequality.

Derivation of $\overline{\kappa}$ for $\kappa_D\to\infty$ and fixed value of $\gamma\rho/\kappa_D$: Because $\gamma\rho$ is infinite, we expect that $x_{-+}=x_{--}=0$, although $z_{-+}\equiv\gamma\rho x_{-+}$ and $z_{--}\equiv\gamma\rho x_{--}$ may converge to positive, though finite, values. Also, because the $+-$ genomes, as conjugators, cannot be "rescued" by conjugators themselves, we expect that $x_{+-}=0$ in the limit as $\kappa_D\to\infty$, although again it is possible that $y_{+-}\equiv\kappa_D x_{+-}$ converges to a positive value. We expect only $x_{++}>0$, since the $++$ genomes are both conjugators and resistant to the antibiotic and so are not destroyed by conjugation or by antibiotic-induced death.

The steady-state equations then become

$$\begin{aligned}\overline{\kappa}&=2p_vp_cp_r-1+(2p_cp_r-1)(z_{-+}+z_{--})\\ y_{+-}&=2p_c(1-p_r)[p_v+z_{-+}+z_{--}]x_{++}\\ z_{-+}&=2(1-p_c)p_r[p_v+z_{-+}+z_{--}]\\ \frac{\kappa_D}{\gamma\rho}z_{--}&=[2(1-p_c)(1-p_r)(p_v+z_{-+}+z_{--})-z_{--}]x_{++}.\end{aligned} \tag{A22}$$

From the first equation we have that $z_{-+}+z_{--}=(\overline{\kappa}+1-2p_vp_cp_r)/(2p_cp_r-1)$. We therefore have that

$$
\begin{aligned}
y_{+-} &= \frac{2p_c(1-p_r)}{2p_cp_r-1}(\overline{\kappa}+1-p_v)x_{++} \\
z_{-+} &= \frac{2(1-p_c)p_r}{2p_cp_r-1}(\overline{\kappa}+1-p_v) \\
z_{--} &= \frac{[1-2p_r(1-p_c)]\overline{\kappa}-[2p_vp_cp_r-1+2p_r(1-p_v)(1-p_c)]}{2p_cp_r-1} \\
\frac{\kappa_D}{\gamma\rho}z_{--} &= \frac{2p_vp_cp_r-1+2(1-p_v)(1-p_c)-(2p_c-1)\overline{\kappa}}{2p_cp_r-1}x_{++}
\end{aligned}
\tag{A23}
$$

and we also have in this limit that $\overline{\kappa} = x_{++} - y_{+-} - \kappa_D/(\gamma\rho)z_{--}$. Substituting in the expressions for y_{+-} and $\kappa_D/(\gamma\rho)z_{--}$, we obtain

$$
x_{++} = \frac{\overline{\kappa}}{\overline{\kappa}+2(1-p_v)}. \tag{A24}
$$

Substituting this expression into the last equality of Equation A23, and using the expression for z_{--}, gives us Equation 9.

Derivation of the transition point between the two functional forms for $\overline{\kappa}$ for $\kappa_D \to \infty$: Equating the finite $\gamma\rho$ with the infinite $\gamma\rho$ expressions for $\overline{\kappa}$, we obtain that the transition point occurs where

$$
\begin{aligned}
&[1-2p_r(1-p_c)]\overline{\kappa}-[2p_vp_cp_r-1+2p_r(1-p_v)(1-p_c)] \\
&\quad = \frac{\overline{\kappa}+1-2p_vp_cp_r}{\sqrt{\kappa_D}} \\
&\qquad \times \sqrt{\frac{2(1-p_r)}{2p_cp_r-1}([2p_vp_cp_r-1+2(1-p_v)(1-p_c)]-(2p_c-1)\overline{\kappa})}.
\end{aligned}
\tag{A25}
$$

Since $\kappa_D \to \infty$, we then obtain that the transition point occurs where the left-hand side is zero, so that $\overline{\kappa} = [2p_vp_cp_r - 1 + 2p_r(1-p_v)(1-p_c)]/[1-2p_r(1-p_c)]$. To estimate the value of $\gamma\rho$ where this transition occurs in the limit of large κ_D, we substitute the expression for $[1-2p_r(1-p_c)]\overline{\kappa}-[2p_vp_cp_r-1+2p_r(1-p_v)(1-p_c)]$ given in Equation A25 into Equation 6 and then substitute the value of $\overline{\kappa}$ that we obtained for the transition. After some manipulation, we obtain the expression given by Equation 11.